

Chapter 4

DNA-binding Py-Im Polyamides Targeted to the AR-ERG Signaling Axis in VCaP Prostate Cancer Cells

The text of this chapter was taken in part from a manuscript draft co-authored with Amanda E. Hargrove, Alissa A. Hare, Jerzy O. Szablowski, and Peter B. Dervan (California Institute of Technology); Sudha Sud (University of Michigan) and Kenneth J. Pienta (Johns Hopkins University).

Abstract

ETS-gene fusions are now recognized as critically important in prostate cancer diagnosis and progression. Specifically, the *TMPRSS2-ERG* fusion results in androgen receptor (AR)-driven overexpression of the ERG protein, a transcription factor which then participates in several oncogenic mechanisms. DNA-binding pyrrole-imidazole (Py-Im) polyamides inhibit transcription factor-DNA interfaces and were thus designed to target the AR-ERG signaling axis through interactions to both AR- and ERG-DNA binding sites. Cell culture studies in VCaP cells, an immortalized cell line harboring the *TMPRSS2-ERG* gene fusion, identified both ARE (AR response element)- and ERG-targeted Py-Im polyamides that significantly downregulate gene expression associated with each respective pathway. Contrary to many DNA-binding small molecule therapeutics, Py-Im polyamides reduced the high levels of double stranded DNA breaks in VCaP cells. Similar cell culture results were observed in the PC3-ERG cell model. Finally, significant reductions in tumor growth were observed in VCaP cell xenografts upon weekly treatment with an ARE-targeted polyamide. These studies support the therapeutic potential of Py-Im polyamides to target ERG-positive prostate cancers without leading to genotoxic stress.

4.1 Introduction

Gene fusions are increasingly recognized as a critical component of prostate cancer progression, in particular fusions involving the E-twenty six (ETS) family of transcription factors (1). Among this family, the *TMPRSS2-ERG* fusion has garnered particular attention due to its prevalence in prostate cancer patient samples (~50%) (2) and its association with aggressive prostate cancers (3,4). The fusion of the 3'-untranslated region of *TMPRSS2*, an androgen receptor (AR) driven gene, and the 5'-translated region of *ERG*, an ETS transcription factor, leads to overexpression of a truncated ERG protein (5). Increased levels of ERG have been associated with a number of oncogenic pathways, including those involved in invasion (6) and DNA damage (7). Furthermore, aberrant ERG expression is sufficient to drive aggressive prostate cancer phenotypes in mouse models when combined with alterations in the pten/PI3K/Akt pathway (8,9).

Pyrrole-imidazole (Py-Im) polyamides bind the minor groove of DNA sequence specifically (Figure 4.1) (10,11), leading to compression of the major groove (12) and offering a unique opportunity to target transcription factor activity. Several oncogenic pathways have been targeted with Py-Im polyamides, and both genotypic and phenotypic responses have been observed in cell culture (13-17) and animal studies (18-20). We recently reported reduction in tumor growth of an LNCaP prostate cancer xenograft upon treatment with a Py-Im polyamide (21). Toxicity studies have revealed a dependence on polyamide architecture in hairpin vs. cyclic polyamides (22) as well as a dependence on differences in hairpin modifications (23,24), allowing for the identification of hairpin

structures demonstrating xenograft growth inhibition but no observed toxicity at 10 mg/kg doses in mice (24). In this study, we show that this technology could be utilized to inhibit both AR signaling, including transcription of the *TMPRSS2-ERG* fusion, and downstream ERG activity in ERG-positive prostate cancer models.

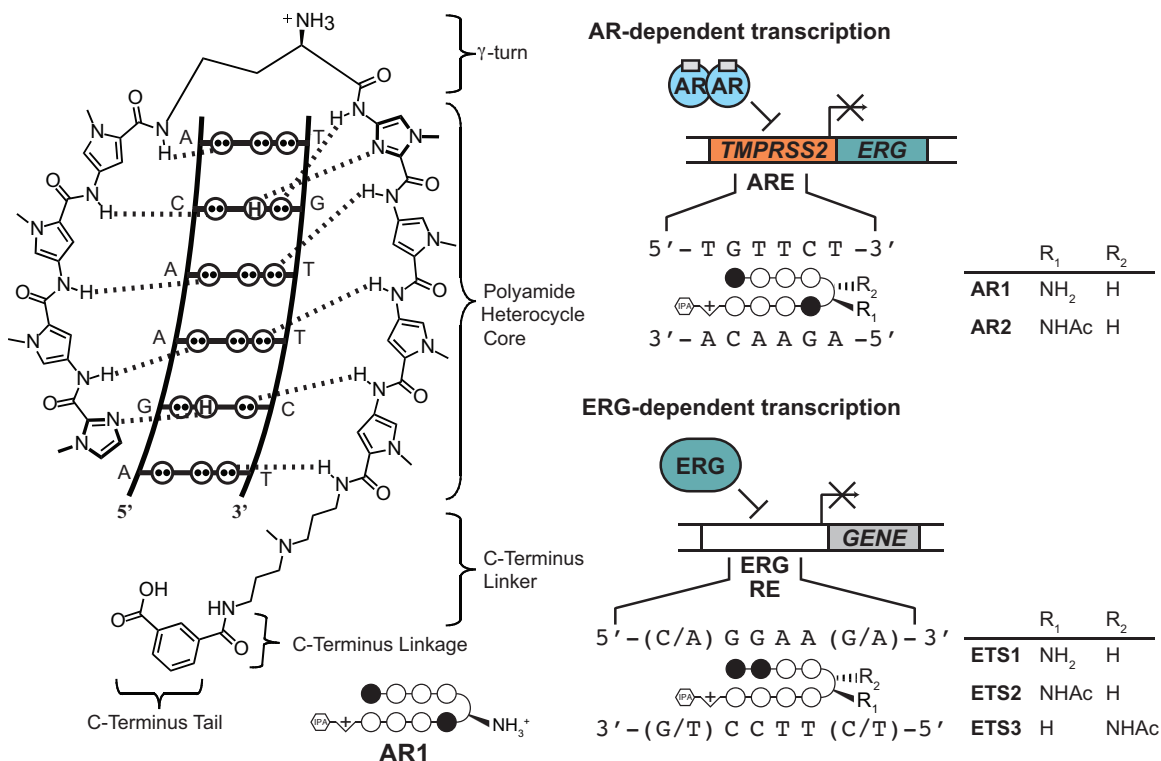




Figure 4.1 Diagrams of targeting AR- and ERG-DNA interfaces by Py-Im polyamides. **(Left)** Model of hairpin Py-Im polyamide recognition of the DNA minor groove in which the Py-Py pair recognizes A·T or T·A base pairs while the Im-Py pair recognizes the G·C base pair. The circle and stick representation (**AR1**) is the shorthand polyamide depiction (code: closed circles, Im; open circles, Py; diamonds, β -alanine; IPA, isophthalic acid). **(Right)** Five Py-Im polyamides used in this study to target prostate cancer cells containing the *TMPRSS2-ERG* gene fusion.

4.2 Results

Design and DNA-binding ability of Py-Im polyamides targeted to the AR-ERG signaling axis.

The two-pronged AR-ERG approach first utilized previously reported Py-Im polyamides **AR1** and **AR2**, which are known to bind the AR response element (ARE) half-site (5'-TGTCT-3') and effect dihydrotestosterone (DHT)-induced expression profiles (14,24), (Table 4.1A). Secondly, a series of Py-Im polyamides was designed to target the ETS-DNA consensus sequence (5'-(C/A)GGAA(G/A)-3'), namely **ETS1**, **ETS2**, and **ETS3** (Figure 4.1). Initial experiments confirmed the ability of the latter set

A					
Sequence		5'-TGTCT-3'			
Polyamide		T_m (°C)	ΔT_m (°C)		
—		61.8 (±0.5)	—		
AR1		74.1 (±0.3)	12.3		
AR2		70.1 (±0.2)	8.3		




B					
Sequence		5'-AGGAAA-3'	5'-AGGAAG-3'	5'-CGGAAG-3'	5'-CGGAAA-3'
T_m (°C)		57.7 (±0.2)	60.1 (±0.4)	58.8 (±0.6)	58.2 (±0.2)
Polyamide		ΔT_m (°C)			
ETS1		8.8 (±0.3)	1.0 (±0.3)	5.9 (±0.2)	7.8 (±0.6)
ETS2		6.6 (±1.0)	0.8 (±0.3)	5.4 (±0.2)	1.6 (±0.6)
ETS3		10.9 (±0.5)	3.7 (±0.4)	7.9 (±0.4)	7.7 (±0.3)

Table 4.1 Analysis of DNA thermal stabilization by binding of Py-Im polyamides. **(A)** Melting temperature analysis for **AR1** and **AR2** binding to match sequence DNA. ΔT_m denotes the shift in melting temperature following the addition of polyamide to the given DNA sequence of the pattern 5'-TTGC-NNNNN-GCAA-3'. Assays were performed at 2 μ M DNA (15 b.p.) with or without 3 μ M polyamide in a buffer solution consisting of 10 mM sodium cacodylate, 10 mM KCl, 10 mM MgCl₂, and 5 mM CaCl₂ at pH 7.0. ΔT_m results for **AR1** and **AR2** are taken from (24). **(B)** Melting temperature analysis for **ETS1-3** binding to match sequence DNA. ΔT_m denotes the shift in melting temperature following polyamide treatment for the given DNA sequence 5'-TGAAA-NNNNN-TGAG-3'.

to bind a variety of potential ERG-DNA binding sequences through thermal denaturation analysis (Table 4.1B).

ARE-targeted Py-Im polyamides mitigate AR-driven TMPRSS2-ERG expression under DHT-induction.

To examine the effect of Py-Im polyamides on AR-driven pathways in ERG-positive cells, the activity of polyamides **AR1** and **AR2** were studied in VCaP cells, the only immortalized cell line known to harbor the *TMPRSS2-ERG* gene fusion. Dosage

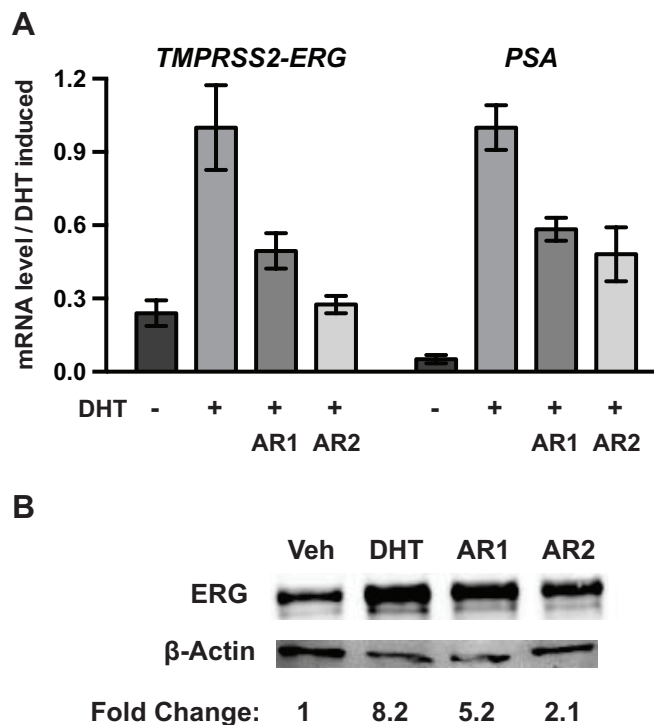


Figure 4.2 Representative expression data for VCaP cells treated with **AR1** and **AR2** followed by DHT-induction. VCaP cells plated at 31k/cm² were treated with medium containing 0.1% DMSO (with or without 10 μ M polHIyamide) and 10% charcoal-treated FBS (CT-FBS) for 72 h followed by induction with 1 nM dihydrotestosterone (DHT) or vehicle for an additional 24 h. **(A)** mRNA expression levels of representative androgen driven genes, *TMPRSS2-ERG* and *PSA*, were measured by qPCR, referenced to *GUSB*, and the polyamide effects compared to vehicle treatment. **(B)** ERG protein levels were measured by immunoblot, referenced to beta-actin, and the polyamide effects compared to vehicle treatment. Gel image has been cropped for clarity.

Treatment	Conc.	DHT	TMP2:ERG	AR	FKBP5	PSA	SLC45A3
Vehicle	-	-	0.23 ± 0.06	2.12 ± 0.19	0.01 ± 0.004	0.07 ± 0.02	0.12 ± 0.04
AR1	10 µM	+	0.50 ± 0.06	0.52 ± 0.13	0.62 ± 0.12	0.63 ± 0.08	0.69 ± 0.18
AR2	1 µM	+	0.68 ± 0.04	0.81 ± 0.17	0.85 ± 0.14	0.77 ± 0.06	0.82 ± 0.34
AR2	10 µM	+	0.30 ± 0.05	0.43 ± 0.08	0.46 ± 0.06	0.47 ± 0.05	0.48 ± 0.13

Treatment	Conc.	DHT	EZH2	MYC	PLAT
Vehicle	-	-	1.08 ± 0.19	12.4 ± 4.06	Unmeasurable
AR1	10 µM	+	1.79 ± 0.46	1.40 ± 0.13	Unmeasurable

Table 4.2 Gene expression data for VCaP cells treated with **AR1** and **AR2** followed by induction with DHT. Data shown are average of the fold changes (normalized to DHT-induced conditions) for three or more biological replicates +/- standard error.

concentrations were chosen based on previous reports of polyamide gene expression effects in the LNCaP prostate cancer cell line (14,24). Both polyamides **AR1** and **AR2** were found to reduce the DHT-induced expression of the *TMPRSS2-ERG* fusion as well as other AR target genes, including *PSA*, in VCaP cells (Figure 4.2, Table 4.2). Decreased expression of ERG protein was confirmed by Western blot (Figure 4.2).

Py-Im polyamides decrease ERG-driven signaling in non-induced VCaP cells.

Polyamides **ETS1**, **ETS2**, and **ETS3** were screened for their effect on ERG-dependent gene expression in VCaP cell culture under non-induced conditions (Figure 4.3, Table 4.3). Notably, all ERG-targeted Py-Im polyamides were observed to downregulate *PLAT*, a well-characterized ERG-driven gene (25), as well as the *MYC* oncogene. While minimal effects were observed on *EZH2* expression, **ETS2** and **ETS3** were found to increase expression levels of *SLC45A3*, a gene reported to be repressed by ERG-DNA binding (26). Due to their ability to inhibit ERG-activated genes and de-inhibit ERG-repressed genes, **ETS2** and **ETS3** were chosen for further phenotypic studies.

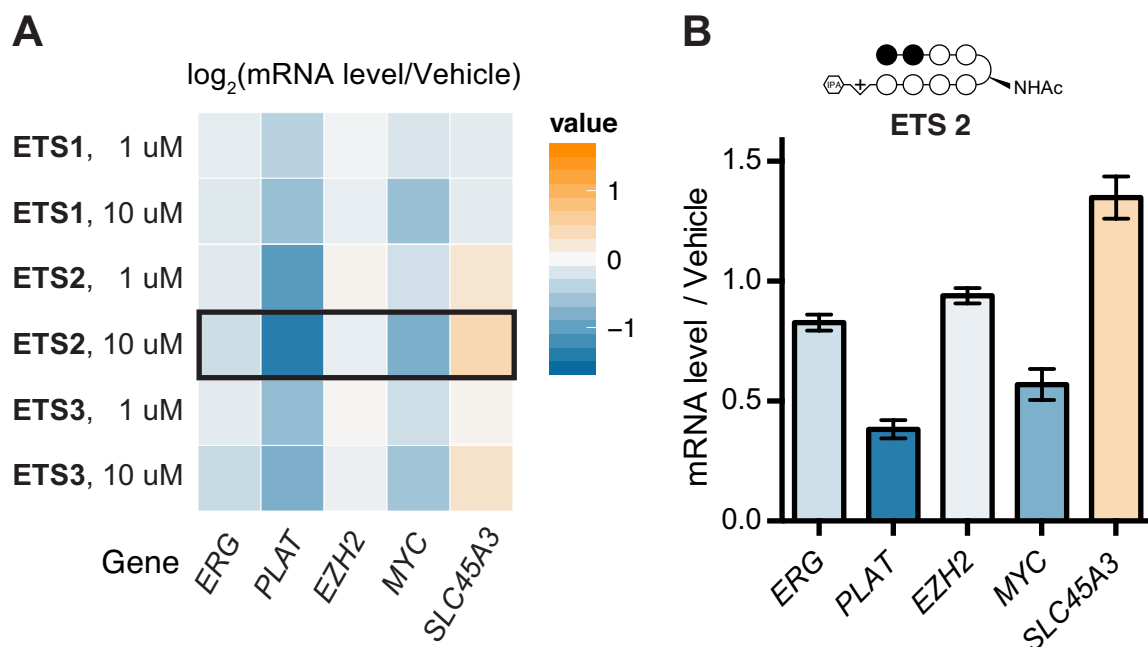


Figure 4.3 Representative expression data for VCaP cells treated with **ETS1-3**. (A) VCaP cells plated at 31k/cm² were treated with medium containing 0.1% DMSO vehicle (with or without polyamide) and 10% FBS for 72 h. mRNA levels were measured by qPCR, referenced to GUSB, and the polyamide effects compared to vehicle treated samples. log₂ conversions of treated/untreated values are reported as a heat map to allow comparison of multiple conditions. (B) Representative data from samples treated with 10 μ M **ETS2**. Bars represent average fold-change of three or more biological replicates \pm standard error.

We also measured the effects of **AR1** and **AR2** on TMPRSS2-ERG expression and downstream targets in VCaP cells under basal conditions. VCaP cells grown in media containing FBS without the addition of DHT. In the absence of DHT-induction, both **AR1** and **AR2** reduced ERG expression, although the effect was less pronounced compared to the effect observed under DHT-induction (Table 4.3). In addition, expression of the ERG-activated genes PLAT and c-Myc were also reduced under treatment with **AR1**.

Polyamide	Conc.	ERG	PLAT	EZH2	MYC	SLC45A3	TMPRSS2-ERG
ETS-1	1 μ M	0.93 \pm 0.02	0.75 \pm 0.10	0.98 \pm 0.05	0.88 \pm 0.02	0.92 \pm 0.02	0.92 \pm 0.04
	10 μ M	0.89 \pm 0.03	0.65 \pm 0.05	0.94 \pm 0.03	0.66 \pm 0.03	0.92 \pm 0.02	0.88 \pm 0.04
ETS-2	1 μ M	0.91 \pm 0.06	0.48 \pm 0.06	1.03 \pm 0.06	0.85 \pm 0.03	1.18 \pm 0.02	0.86 \pm 0.08
	10 μ M	0.83 \pm 0.03	0.38 \pm 0.04	0.94 \pm 0.03	0.57 \pm 0.07	1.35 \pm 0.09	0.80 \pm 0.05
ETS-3	1 μ M	0.93 \pm 0.02	0.64 \pm 0.07	1.01 \pm 0.05	0.83 \pm 0.03	1.04 \pm 0.09	0.94 \pm 0.02
	10 μ M	0.80 \pm 0.03	0.57 \pm 0.05	0.96 \pm 0.05	0.68 \pm 0.06	1.21 \pm 0.10	0.89 \pm 0.05
AR-1	1 μ M	0.84 \pm 0.07	0.67 \pm 0.06	1.00 \pm 0.10	0.70 \pm 0.04	0.98 \pm 0.10	1.02 \pm 0.08
	10 μ M	0.86 \pm 0.05	0.42 \pm 0.11	0.93 \pm 0.03	0.49 \pm 0.05	0.78 \pm 0.07	0.91 \pm 0.05
AR-2	1 μ M	0.67 \pm 0.06	0.68 \pm 0.09	1.03 \pm 0.07	0.66 \pm 0.06	0.56 \pm 0.06	0.66 \pm 0.06
	10 μ M	0.49 \pm 0.04	0.46 \pm 0.02	0.89 \pm 0.03	0.32 \pm 0.02	0.29 \pm 0.03	0.50 \pm 0.04

Polyamide	Conc.	AR	PSA	FKBP5
AR-1	1 μ M	0.96 \pm 0.04	0.81 \pm 0.09	0.93 \pm 0.09
	10 μ M	1.09 \pm 0.08	0.68 \pm 0.08	0.83 \pm 0.04
AR-2	1 μ M	0.87 \pm 0.04	0.66 \pm 0.02	0.81 \pm 0.02
	10 μ M	0.75 \pm 0.05	0.49 \pm 0.07	0.46 \pm 0.03

Table 4.3 Gene expression data for VCaP cells treated with ETS-targeting and AR-targeting polyamides. Data shown are average of the fold changes (normalized to DHT-induced conditions) for three or more biological replicates \pm standard error.

Cytotoxicity and nuclear uptake of Py-Im polyamides.

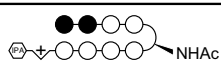
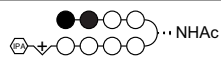
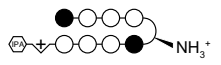
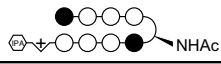
The four lead molecules, **ETS2**, **ETS3**, **AR1**, and **AR2**, were further examined for effects on proliferation of VCaP cells using the WST-1 assay under conditions similar to the gene expression experiment. After a 72 h incubation with polyamide, an IC_{50} value of $12 \pm 2 \mu$ M was determined for **AR2** but the remaining molecules did not reach a 50% reduction in signal at concentrations below 30 μ M, above which polyamide aggregation began to be observed (Figure 4.4). In contrast, **AR1** has been found to have an IC_{50} of $7 \pm 3 \mu$ M under similar conditions in LNCaP cells (21). When incubated for 96 h, however, **AR** was found to have an IC_{50} of $6.5 \pm 0.3 \mu$ M. To test differences in uptake, FITC-labeled derivatives of each lead molecule were prepared and incubated with VCaP cells prior to imaging by confocal microscopy (Figure 4.5,4.6). All intracellular polyamide signal was observed to be localized in the nucleus, with **ETS3-FITC** and **AR1-FITC**

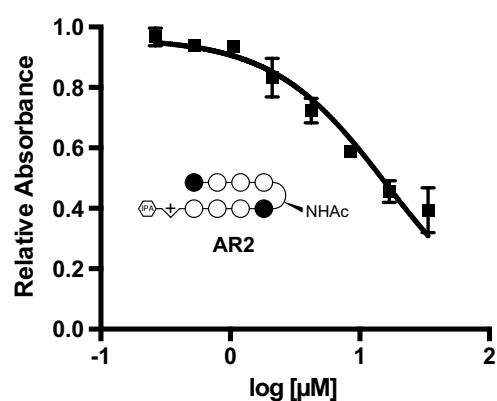
also showing significant membrane binding. In line with the cytotoxicity results, **AR2-FITC** displayed the strongest nuclear uptake. The overall level of uptake in VCaP cells was found to be qualitatively less than that in LNCaP cells (24).

Reduction of DNA damage in VCaP cells upon treatment with Py-Im polyamides.

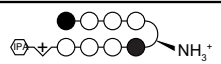
The effect of DNA-binding polyamides on the high level of extant DNA damage in VCaP cells was also investigated. After incubation with polyamide, VCaP cells were submitted to the neutral Comet assay, which allows visualization of double-strand breaks

A

Py-Im Polyamide	IC ₅₀ (WST-1)
ETS2 	> 30 μ M
ETS3 	> 30 μ M
AR1 	> 30 μ M
AR2 	12 \pm 3 μ M



B

Py-Im Polyamide	IC ₅₀ (WST-1)
AR1 	6.5 \pm 0.3 μ M

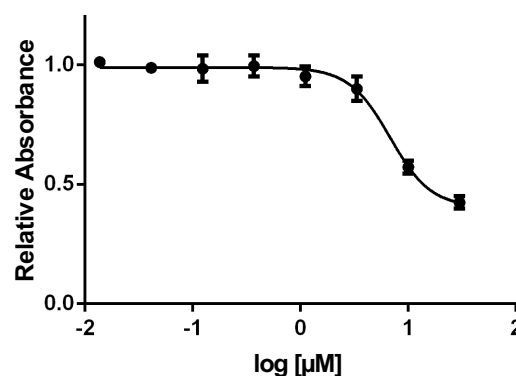


Figure 4.4 AR1 and AR2 are cytotoxic in VCaP cells. (A) Cytotoxicity (IC₅₀) values were determined using the WST-1 assay after 72 h incubation of VCaP cells with Py-Im polyamide. The conversion of WST-1 to formazan was measured by the absorbance at 450 nm referenced to 650 nm in treated cells and compared to that of vehicle (0.1% DMSO) treated cells. Top: Values are reported as the average \pm SEM of three or more biological replicates where applicable. Bottom: Representative data from a single replicate using polyamide **AR2**. (B) WST-1 assay results after 96 h incubation of VCaP cells with **AR1**.

through single cell electrophoresis (Figure 4.7). The percentage of DNA in the “tail” of the comets was then compared using two-way ANOVA statistical analysis. A significant reduction in DNA damage ($p < 0.001$) was observed with **ETS2**, **ETS3**, and **AR1** over the vehicle control. No significant difference was observed upon treatment with **AR2**, possibly due to competing effects of toxicity. Interestingly, treatment with **ETS3** led to notably reduced damage relative to the other polyamides tested ($p < 0.001$ vs **ETS2** and

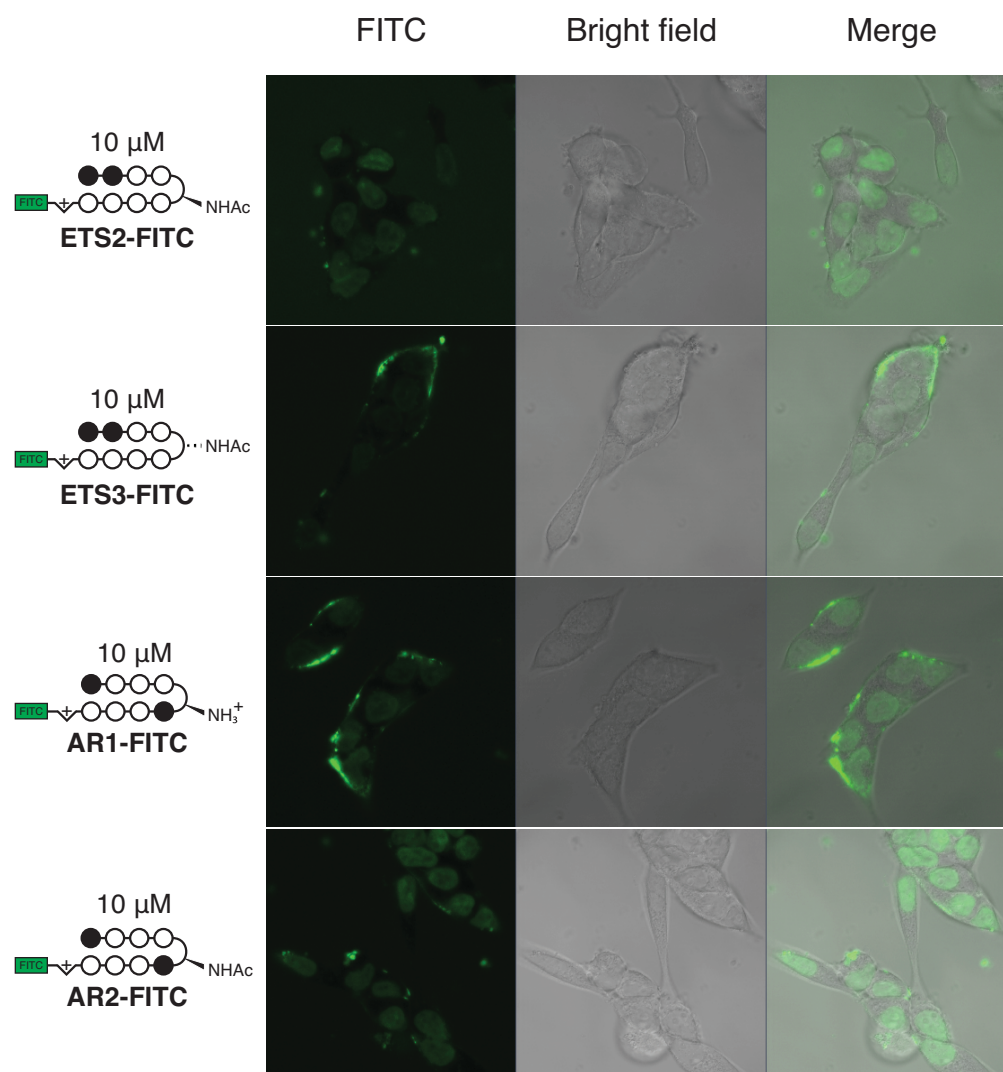


Figure 4.5 Nuclear uptake of FITC-analog polyamides in VCaP cells after 24 h. VCaP cells seeded at a density of 300,000/mL were incubated with FITC-labeled polyamides for 24 h before visualization by confocal microscopy. **ETS2** and **AR2** show significant nuclear uptake, while other compounds tested showed significant membrane binding but relatively low nuclear uptake.

AR1, respectively), despite the modest level of cellular uptake observed with the FITC-derivative (Figure 4.5,4.6) and the weaker effects on ERG-related gene expression compared to **ETS2** (Figure 4.3). At the same time, **ETS3** did stabilize the cognate ERG-DNA binding sequence to a greater extent than **ETS2** (Table 4.1), which may indicate a dependence on DNA stabilization in the reduction of double stranded breaks.

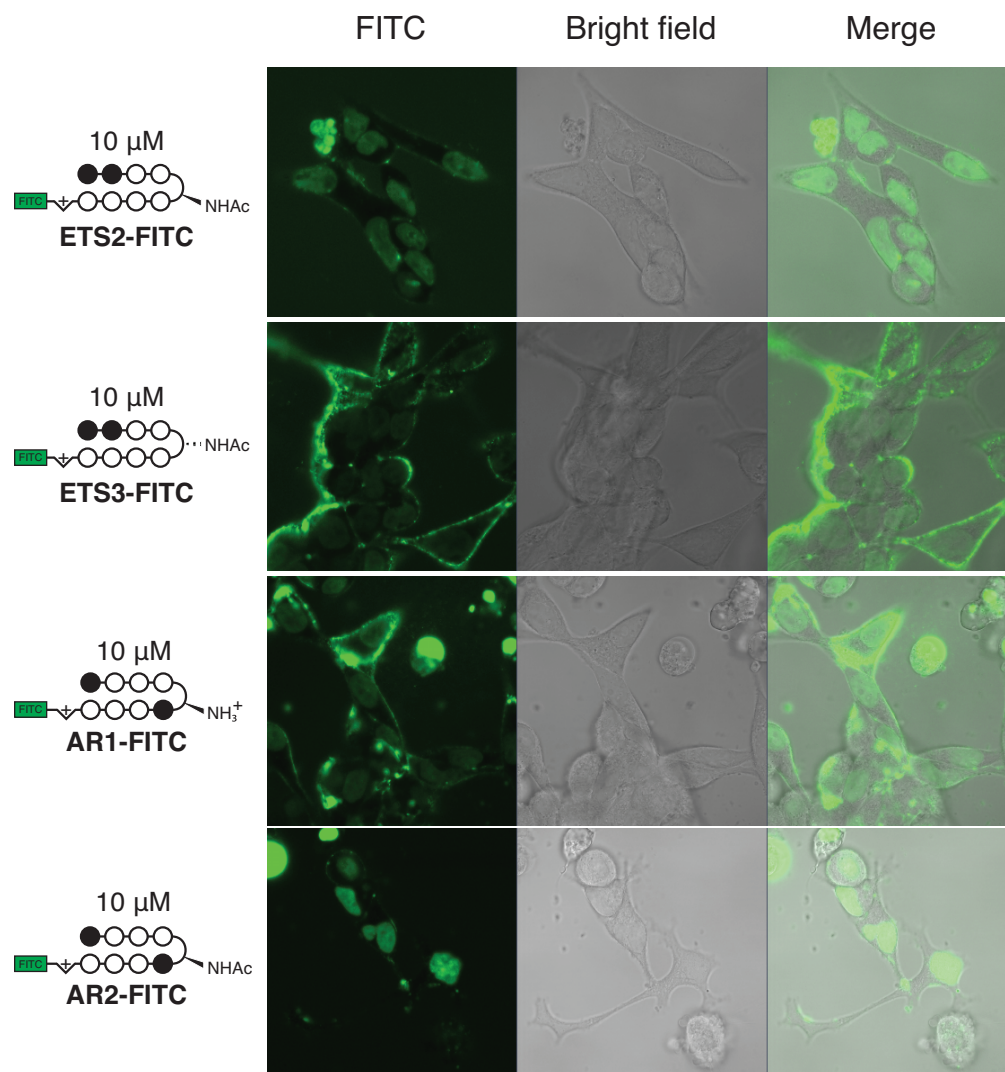


Figure 4.6 Nuclear uptake of FITC-analog polyamides in VCaP cells after 48 h. VCaP cells seeded at a density of 300,000/mL were incubated with FITC-labeled polyamides for 48 h before visualization by confocal microscopy. **ETS2** and **AR2** show significant nuclear uptake, while other compounds tested showed significant membrane binding but relatively low nuclear uptake.

Py-Im polyamide activity in PC3 cells overexpressing ERG.

Polyamide effects were further studied in the PC3-ERG cell line, which was derived from the AR- and ERG-negative PC3 prostate cancer line (7,27). Comparing PC3-ERG to the direct parent cell line, PC3-Luc, the strongest differences in expression were observed in the upregulation of *PLAT* and downregulation of *SLC45A3* (Figure 4.8, 4.9). Polyamides **ETS2** and **ETS3**, as well as control polyamide **AR1**, were chosen for comparison due to their observed lack of toxicity in VCaP cells. Treatment with all three polyamides resulted in expression levels of *PLAT* and *SLC45A3* near the parent levels, with **AR1** demonstrating the strongest activity. Significant reductions in DNA damage were also observed in Comet assays of PC3-ERG cells upon treatment with **ETS3** and **AR1** ($p < 0.001$). Notably, **AR1** decreased overall *ERG* expression nearly 2-fold, an

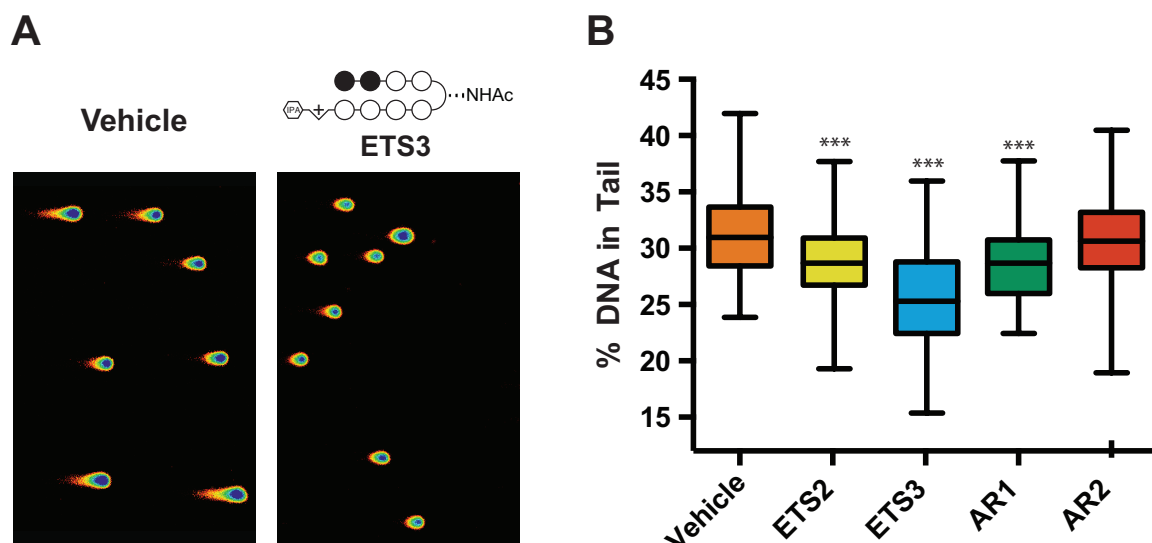


Figure 4.7 Analysis of DNA damage by neutral comet assay. (A) The extent of DNA damage in untreated and treated VCaP cells was measured using the neutral COMET assay after 72 h incubation with 0.1% DMSO (vehicle) with or without 10 μ M Py-Im polyamide as indicated. Comets were analyzed using Comet Assay IV software (Perceptive). Statistical significance was determined using two-way ANOVA analysis (Prism) where *** = $p < 0.001$ relative to vehicle. Boxes are bounded by the upper and lower quartile, while whiskers represent the 1st and 99th percentile. (B) Representative images taken for vehicle and ETS2 treated cells.

unexpected effect given the CMV promoter driving its overexpression. The significant effects of **AR1** on *PLAT* and *SLC45A3* expression (Figure 4.9) as well as the reduction in DNA damage levels in PC3-ERG cells suggest a general rather than ERG-specific mechanism for this molecule.

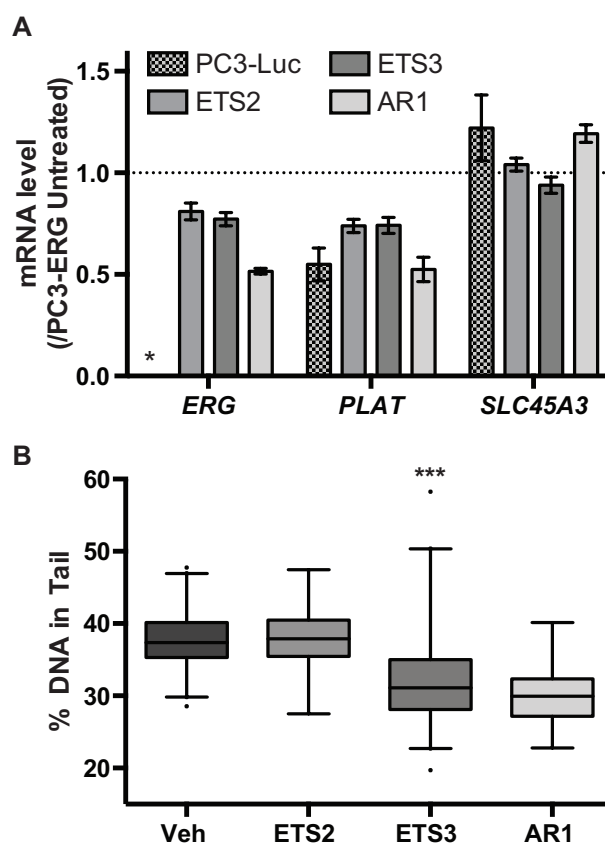


Figure 4.8 Py-Im polyamides mediate ERG-driven expression in PC3-ERG cells and reduce extant DNA damage. **(A)** PC3-ERG cells were treated with 0.1% DMSO (with or without 10 μ M polyamide) for 72 h. mRNA levels were measured by qPCR and referenced to GUSB. *ERG mRNA levels were too low to be measured in PC3-Luc cells. **(B)** The extent of DNA damage in untreated and treated PC3-ERG cells was measured using the neutral COMET assay. Comets were analyzed using Comet Assay IV software (Perceptive). Statistical significance was determined using two-way ANOVA analysis (Prism) where *** = $p < 0.001$ relative to vehicle. Boxes are bounded by the upper and lower quartile, while whiskers represent the 1st and 99th percentile, and outliers are indicated by single points.

Tube formation studies in a healthy cell line model.

Preliminary investigations of polyamide effects on ERG-activity in healthy cells involved the study of tube formation in human umbilical vein endothelial cells (HUVEC) as this process has been reported to be driven by ERG (28). After incubation with polyamide, **ETS2**, **ETS3**, and **AR1** demonstrated no significant effects on tube formation. Treatment with **AR3**, however, led to a nearly 2-fold reduction in observable branching points (Figure 4.10). The reduction observed upon treatment with **AR2** was unexpected and inhibition of angiogenesis will be investigated as a potential side effect of **AR2** treatment.

	PLAT	PLAU	SLC45A3	ERG	EZH2	MYC
PC3-Luc (control)	0.55 ± 0.05	1.24 ± 0.02	1.22 ± 0.09	0.00 ± 0.30	0.99 ± 0.04	1.32 ± 0.06
ETS2	0.74 ± 0.03	0.88 ± 0.03	1.04 ± 0.03	0.81 ± 0.04	1.01 ± 0.02	0.94 ± 0.04
ETS3	0.74 ± 0.04	0.79 ± 0.02	0.94 ± 0.04	0.77 ± 0.03	0.99 ± 0.02	0.96 ± 0.04
AR1	0.52 ± 0.06	0.53 ± 0.05	1.19 ± 0.04	0.52 ± 0.01	1.08 ± 0.04	1.32 ± 0.05

Figure 4.9 Gene expression data for PC3-ERG cells treated with ETS-targeting and AR-targeting polyamides for 72 h. Data shown are average of the fold changes (normalized to expression levels in PC3-ERG cells) for three or more biological replicates +/- standard error.

Diminished growth in VCaP xenografts upon polyamide treatment.

Initial xenograft experiments were conducted with **AR1** and **ETS3** in male SCID mice bearing subcutaneous VCaP cell xenografts. Treatments were started after tumor sizes in each group of mice reached ~100 mm³ and were administered three times per week for a total of 10 injections through subcutaneous injection in DMSO vehicle. Dose-dependent retardation of tumor growth was observed in mice treated with **AR1** (Figure 4.11). After 5 weeks, tumors treated with vehicle grew to approximately 6-fold the initial volume of that group while tumors treated with **AR1** at 5.0 mg/kg grew to approximately 1.6-fold the initial volume of that cohort. Equivalent treatment with **ETS3**, however, did not exhibit this effect.

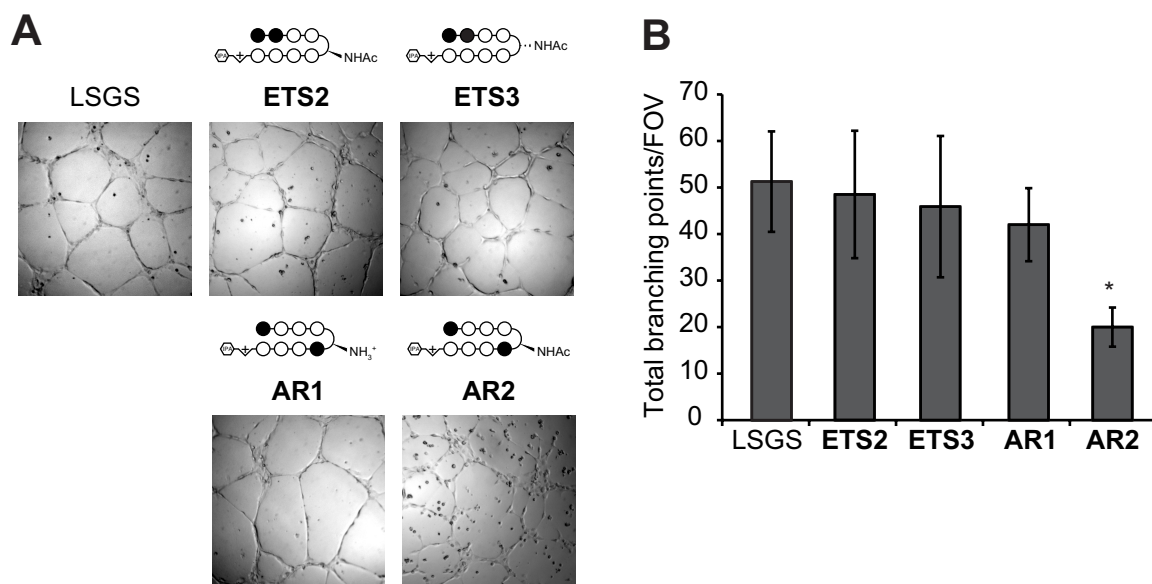


Figure 4.10 AR2 inhibits HUVEC tube formation *in vitro*. (A) Representative images showing effects of Py-Im polyamides (10 μ M) on the formation of tubes by HUVEC cells after 72 h incubation. Only AR2 demonstrated perturbed tube formation resulting in a fragmented network. (B) Quantitative analysis of branching points show that AR2 significantly inhibited tube formation in this assay * = $p < 5e-4$. A total of 8 fields of view, split between 4 different wells were been used in this data. Error bars represent 95% CI.

4.3 Discussion

This study evaluated the ability of Py-Im polyamides to target oncogenic pathways in advanced prostate cancer, specifically the AR-ERG signaling axis. Effects on gene expression, DNA damage levels, and *in vivo* tumor growth were observed VCaP cells, which express high levels of AR and the *TMPRSS2-ERG* gene fusion, as well as PC3-ERG cells, which is derived from PC3 prostate cancer cells that are natively AR- and ERG. The activity of Py-Im polyamides AR1 and AR2 targeting the ARE, had been previously studied in LNCaP cells, a model of castration-resistant prostate cancer that is AR-positive but ERG-negative (14,24). Polyamides were designed to target the ERG-DNA consensus sequence following the traditional Py-Im pairing rules (Figure 4.1). Substitution at the turn position was varied based on reports of its importance to cell

culture activity and *in vivo* toxicity (24). **ETS1** and **ETS3** have been previously studied in A549 cells for effects on the NF- κ B pathway (17,18) while **ETS2** is a novel molecule. The ability of these molecules to bind potential ERG-DNA binding sites was confirmed through thermal denaturation analysis prior to cell culture work (Table 4.1B).

Initial cell culture experiments determined that ARE-targeted polyamides **AR1** and **AR2** were able to disrupt DHT-induced signaling in VCaP cells, in line with previous studies in LNCaP cells (Figure 4.2, Table 4.2) (14,24). Decreased levels of the *TMPRSS2-ERG* fusion transcript were observed after polyamide treatment as well as reduced levels of ERG protein expression by Western blot (Figure 4.2). We also observed downregulation of other known AR targets, *PSA* and *FKBP5* (Table 4.2). Interestingly, **AR1** and **AR2** still had a small effect on *ERG* expression and the downstream targets *PLAT* and *c-Myc* under non-DHT-induced conditions (Table 4.3). Given the decrease in transcription by polyamides, as polyamide treatment has been shown to cause RNA pol II

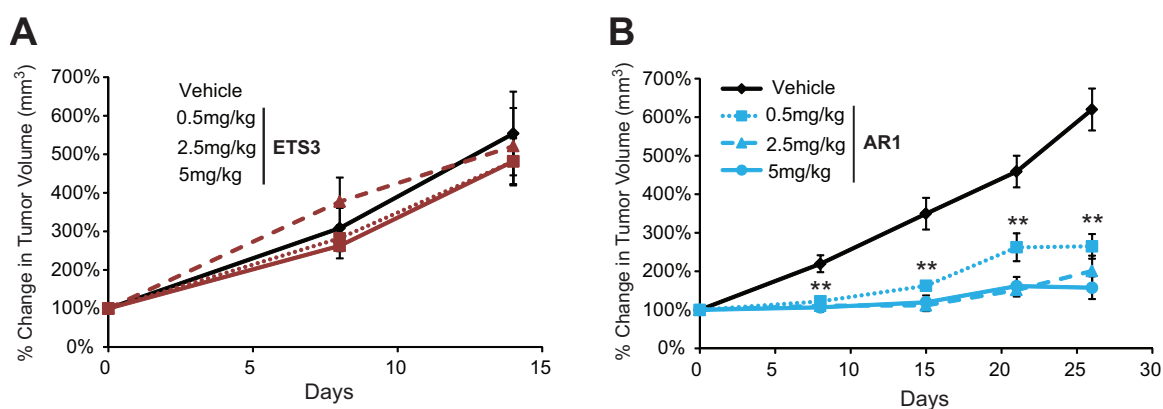


Figure 4.11 **AR1** but not **ETS3** reduces the growth of VCaP tumors in SCID mice. VCaP tumors were measured by caliper and treatment began when the tumor size reached 100 mm³. All mice were treated subcutaneously with vehicle (DMSO) or (A) **ETS3** or (B) **AR1** as reported (3 times per week, 10 total injections). Tumor growth was followed weekly by caliper measurements. All data points were measured in groups of 6-10 mice except for the week 4 data point of ETS3 treatment in which all but 2 mice had to be euthanized due to large tumor size.

ERG expression is fairly low, this result may reflect a non-specific or general effect on degradation previously (21). Furthermore, Py-Im polyamides targeted to the *ERG*-DNA binding site reversed the effects of *ERG* overexpression on select genes (Figure 4.3), despite the modest uptake in VCaP cells observed with the FITC-conjugates (Figure 4.5,4.6). These studies confirmed that Py-Im polyamides have the potential to affect the AR-*ERG* signaling axis in prostate cancers natively expressing the gene fusion.

Given the positive results observed on gene expression, we wanted to probe for polyamide effects on *ERG*-driven phenotypes. *ETS* gene fusions in prostate cancer are thought to be formed by double stranded DNA breaks at transcription factor-targeted loci (29) and overexpression of *ETS* proteins has been observed to increase the prevalence of double stranded DNA breaks (7,27). While these breaks ultimately result in cancer cell death, increases in the number of DNA breaks may also lead to higher mutational rates in prostate cancer (1). Consistent with the downregulation of *ERG* expression and downstream targets, treatment with **ETS2**, **ETS3**, and **AR1** caused a reduction in double stranded DNA breaks in VCaP cells (Figure 4.7). This result is in contrast to other DNA-binding therapeutics, such as the TOP2B inhibitors etoposide and doxorubicin, which lead to increased levels of DNA breaks. While these breaks ultimately result in cancer cell death, increases in the number DNA breaks may also lead to higher mutational rates in prostate cancer (1). Py-Im polyamides, which participate in non-covalent interactions with DNA, may thus present a unique route to therapeutically target DNA without increasing, and in some cases decreasing, levels of double stranded DNA breaks in cancer cells. Investigations are underway to determine the underlying cause of this

decreased DNA damage, specifically whether it is the result of disrupted ERG-DNA interactions or a combination with more general mechanisms of polyamide activity.

Genotypic and phenotypic effects were also observed in the PC3-ERG cell line, created as an isogenic cell line to PC3 cells, which do not express AR or ERG. Specifically, polyamides **ETS2**, **ETS3**, and **AR1** demonstrated significant decreases in ERG-driven gene expression, and a reduction in DNA damage was also observed with **ETS3** and **AR1** (Figure 4.8,4.9). Though formally targeted to the ARE, **AR1** was found to be the most effective at reversing ERG-related effects on mRNA levels. The strong decrease in DNA damage by **AR1** in PC3-ERG cells was also unexpected. In this system, **AR1** is as effective as **ETS3** in reduction of DNA damage, though **ETS3** was found to be more effective than all other polyamides in VCaP cells. These results are consistent with an overall decrease in ERG protein levels by **AR1**, a hypothesis supported by the strong downregulation of *ERG* mRNA levels after **AR1** treatment. This downregulation may indicate binding of **AR1** to the CMV promoter rather than native transcription factor binding sites or general inhibition of transcription.

We also investigated the effect of polyamides on another ERG-driven phenotype, tube formation in human umbilical vein endothelial cells (HUVECs). **ETS2**, **ETS3**, and **AR1** showed no effect on the ability of HUVECs, a model of healthy cells, to undergo tube formation (Figure 4.10). These results suggest that the ERG-targeting polyamides may not have significant effects in healthy cells, which would be an advantage as a potential therapeutic. Interestingly, treatment with **AR2** inhibited tube formation in

HUVECs, despite the ERG coding region not being fused to the AR-driven promoter of TMPRSS2 as in VCaP cells. Inhibition of tube formation only occurring in response to **AR2** is also consistent with the high potency observed in gene expression and cytotoxicity assays, and suggests that this compound might act non-specifically.

To further investigate the therapeutic potential of Py-Im polyamides against ERG-positive prostate cancer, **AR1** and **ETS3** were tested for efficacy against VCaP xenografts in SCID mice. Weekly treatment with **AR1** at 5.0 mg/kg resulted in a notable reduction in tumor growth relative to vehicle treated controls (Figure 4.11) with no observable signs of toxicity. A similar reduction in tumor growth was not observed in **ETS3** treated mice. This result is consistent with the cytotoxicity of **AR1** observed in cell culture and the downregulation of ERG and downstream targets given that ERG is a driver of cell proliferation in VCaP cells (30). It is possible, however, that general effects on transcription or replication by **AR1** may also contribute to the observed reduction in tumor growth (21,31). Reduced tumor growth and the observed reduction in expression of ERG targets in both the presence and absence of DHT-induction also suggest that **AR1** can be effective even when circulating levels of androgens are low. Why **ETS3** showed no effect is unclear, though this molecule also failed to reduce the growth of A549 xenografts in SCID mice despite showing toxicity in cell culture (32). Therefore, there is likely a confounding variable that contributes to the efficacy of polyamides against mouse xenografts, such as uptake into engrafted cells (33), that is not captured by cell culture studies. Subsequent studies will focus on higher doses of these molecules to

determine the therapeutic window as well as examination of the *in vivo* activity of second-generation compounds **AR2** and **ETS2**.

In conclusion, these studies indicate that select Py-Im polyamides can be used to reverse many of the negative effects of AR and ERG related signaling in prostate cancer, including oncogenic expression pathways and DNA damage, while also slowing tumor growth in an AR- and ERG-positive prostate cancer xenograft. Future work will focus on detailed mechanistic studies as well as non-rodent toxicity studies as we push to determine the utility of this class of molecules in human therapeutics.

4.4 Materials and Methods

Synthesis and quantitation of Py-Im polyamides.

All synthesis was performed using previously reported procedures as indicated (34,35). Chemicals were obtained from Sigma Aldrich or Fisher Scientific unless otherwise noted. Briefly, polyamides were synthesized by microwave-assisted solid phases synthesis on Kaiser oxime resin (Nova Biochem) (34) and then cleaved from the resin with neat 3,3'-diamino-*N*-methyldipropylamine. The triamine-conjugated polyamides were purified by reverse phase HPLC and subsequently modified at the C-terminus with isophthalic acid (IPA) or fluorescein-5-isothiocyanate (FITC isomer I, Invitrogen) (35). The α - or β -amine substituents of the γ -aminobutyric acid (GABA) turn units of the polyamides were deprotected using either trifluoroacetic acid (Boc) or 9:1 trifluoroacetic acid/triflic acid (CBz), respectively (36,37). For polyamides **AR2**, **ETS2**, and **ETS3**, the primary amine on the turn unit was acetylated using excess acetic

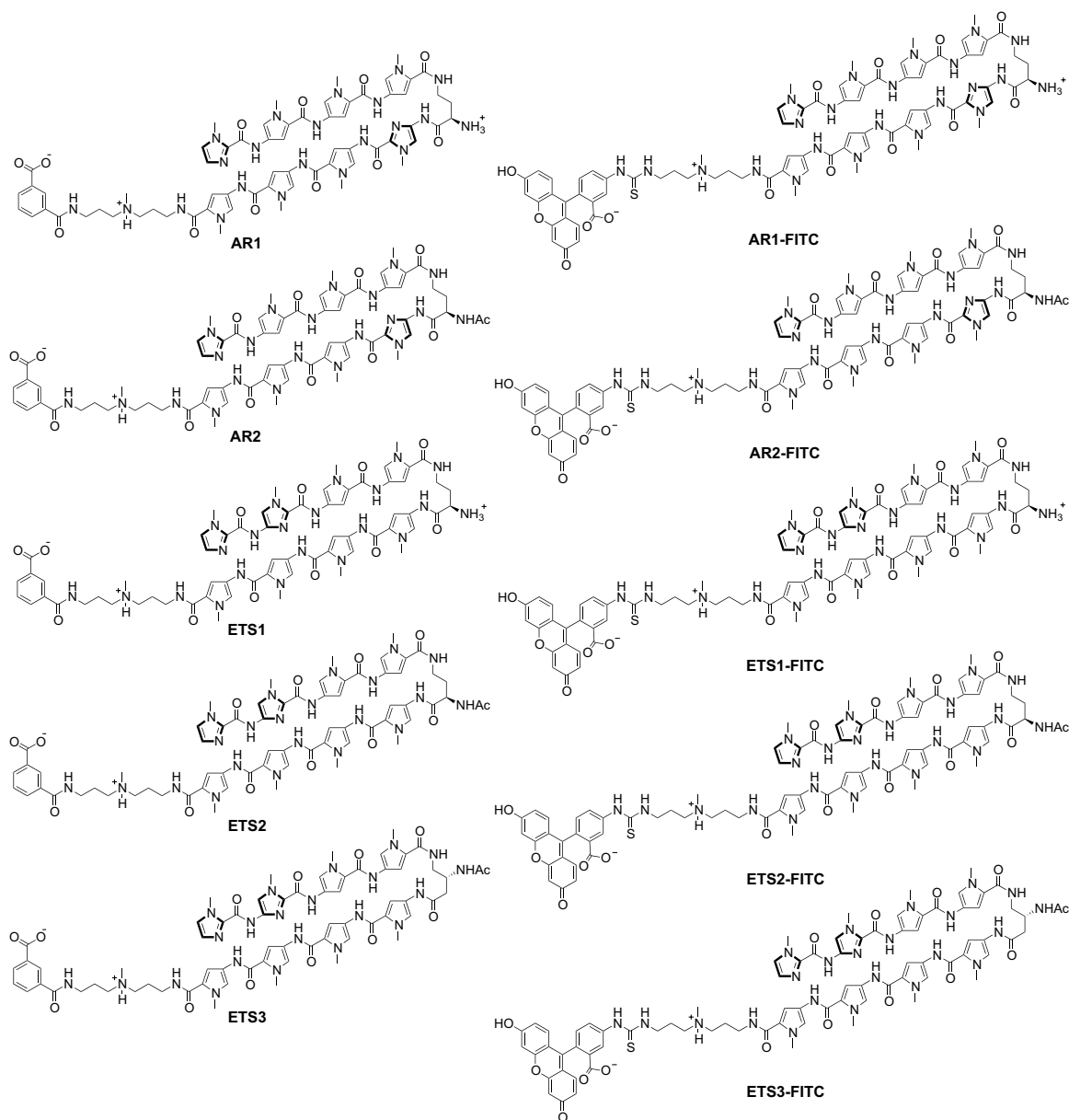


Figure 4.12 Chemical structures of Py-Im polyamides studied.

anhydride under basic conditions (38). The final polyamides were purified by reverse phase HPLC, lyophilized to dryness, and stored at -20°C . The identity and purity of the final compounds were confirmed by matrix-assisted, LASER desorption/ionization time-of-flight (MALDI-TOF) spectrometry and analytical HPLC. Chemical structures are represented in Figure 4.12.

Py-Im polyamides were dissolved in sterile DMSO (ATCC) and quantitated by UV spectroscopy in either 4:1 0.1% TFA (aqueous):acetonitrile ($\epsilon(310\text{nm}) = 69,500 \text{ M}^{-1}\text{cm}^{-1}$) or 9:1 water:DMSO ($\epsilon(310\text{nm}) = 107,100 \text{ M}^{-1}\text{cm}^{-1}$) as dictated by solubility. Polyamides were added to cell culture solutions at 10x concentration to give 0.1% DMSO solutions.

Thermal denaturation analysis.

Melting temperature analysis was carried out using a Varian Cary 100 spectrophotometer with a thermocontrolled cell holder and a cell path length of 1 cm. The analysis buffer used was a degassed aqueous solution of 10 mM sodium cacodylate, 10 mM KCl, 10 mM MgCl_2 , and 5 mM CaCl_2 at pH 7.0. Oligonucleotides were purchased from Integrated DNA technologies (HPLC purified) and were added as a 200 μM solution in Ultrapure Distilled Water (Gibco). DNA duplexes and polyamides were mixed to a final concentration of 2 μM and 3 μM , respectively, in 1 mL of analysis buffer just prior to each experiment. The samples were initially heated to 90°C and then cooled to 25°C. The denaturation profiles were recorded at $\lambda = 260 \text{ nm}$ from 25°C to 90°C with a heating rate of 0.5°C/min. The melting temperatures were defined as the maximum of the first derivative of the denaturation profile.

Cell culture.

All cell lines were obtained from the laboratories of Dr. Kenneth J. Pienta and Dr. Arul M. Chinnaiyan at the University of Michigan Department of Pathology. VCaP cells

were received at passage 19 and cultured in DMEM (Gibco 10313-039) with 4 mM glutamine (Invitrogen) and fetal bovine serum (Omega Scientific) on Corning CellBind flasks. All experiments were performed below passage 30. PC3 cells expressing luciferase (PC3-Luc) or expressing luciferase and the *TMPRSS2-ERG* gene fusion (PC3-ERG) have been previously described (7,27) and were cultured in RPMI medium (Gibco, 21870-092).

Gene expression analysis by quantitative RT-PCR (qPCR).

For dihydrotestosterone (DHT) induction experiments, VCaP cells were plated in 6-well plates coated with poly-L-lysine (BD BioCoat) in charcoal-treated FBS containing media at a density of $31\text{k}/\text{cm}^2$ (3×10^5 cells per well). The cells were allowed to adhere for 24 h and then dosed with 0.1% DMSO with or without polyamide for 72 h followed by the addition of 0.01% ethanol in PBS with or without dihydrotestosterone (1 nM final concentration). Cells were harvested after additional 24 h incubation. For native expression experiments, VCaP cells were plated as above but using standard FBS media and harvested after 72 h of treatment. PC3-Luc and PC3-ERG cells were plated in 6-well plates without poly-L-lysine at 2.5×10^4 cells per well and allowed to adhere for 24 h before treatment with 0.1% DMSO, with or without polyamide, for 72 h. For all experiments, the mRNA was extracted using the QIAGEN® RNeasy mini kit following the standard purification protocol. Samples were submitted to DNase treatment using the TURBO DNA-free Kit (Ambion), and the mRNA was reverse-transcribed by using the Transcriptor First Strand cDNA Synthesis Kit (Roche). Quantitative PCR was performed by using the FastStart Universal SYBR Green Master (Rox) (Roche) on an ABI 7300

qPCR (mRNA)	Sequence	Reference
AR-f	CAGTGGATGGGCTGAAAAAT	Yu JD, et al. Cancer Cell. 2010;17:443-54.
AR-r	GGAGCTTGGTGAGCTGGTAG	
cMYC-f	AGCGGGCGGGCACTTTGC	*
cMYC-r	GCGGGAGGCTGCTGGTTTTTC	
ERG_ALL-f	CGCAGAGTTATCGTGCCAGCAGAT	Tomlins SA, et al. Science. 2005;310:644-8.
ERG_ALL-r	CCATATTCTTTCACCGCCCACTCC	
EZH2-f	TGCAGTTGCTTCAGTACCCATAAT	Yu JD, et al. Cancer Cell. 2010;17:443-54.
EZH2-r	ATCCCCGTGTACTTTCCCATCATAAT	
FKBP5-F	CGG AAA GGA GAG GGA TAT TCA	Meier JL, et al. Nucleic Acids Res. 2011;40:2345-56.
FKBP5-R	CCA CAT CTC TGC AGT CAA ACA	
GUSB-f	CTCATT TGGAATTTTGCCGATT	Jacobs CS, et al. J Med Chem. 2009;52:7380-8.
GUSB-r	CCGAGTGAAGATCCCCCTTTTA	
KLK3-f	TCTGCGGCGGTGTTCTG	Jacobs CS, et al. J Med Chem. 2009;52:7380-8.
KLK3-r	GCCGACCCAGCAAGATCA	
PLAT-f	GCAGAGCCCTCTCTTCATTG	*
PLAT-r	CTGGAGAGAAAACCTCTGCG	
PLAU-f	CCAGCTCACAATTCCAGTCA	*
PLAU-r	TGACCCACAGTGGAAAACAG	
SLC45A3-f	TCGTGGGCGAGGGGCTGTA	Lin C, et al. Cell. 2009;139:1069-83.
SLC45A3-r	CATCCGAACGCCTTCATCATAGTGT	
TMPRSS2-ERG-f	TAGGCGCGAGCTAAGCAGGAG	Tomlins SA, et al. Science. 2005;310:644-8.
TMPRSS2-ERG-r	GTAGGCACACTCAAACAACGACTGG	

Figure 4.13 Primer sequences for qPCR analysis. Sequences for mRNA analysis without a listed reference (*) were designed using qPrimerDepot (primerdepot.nci.nih.gov), and the single amplification products verified by agarose gel electrophoresis against the 1.1 kB NEB ladder.

Real Time PCR System. Gene expression was normalized against GUSB. Primers used are referenced in Figure 4.13.

Immunoblot of ERG protein levels.

For assessment of ERG and beta-actin protein levels, 3×10^6 VCaP cells were plated in 10 cm diameter dishes with charcoal-treated FBS containing media for 24 h before treatment with 0.1% DMSO vehicle with or without **AR1** or **AR2** for an additional 72 h. Ethanol (0.01%) in PBS with or without dihydrotestosterone (1 nM final concentration) was then added. After 24 h incubation, cells were lysed in TBS-Tx buffer (50 mM Tris-HCl pH 7.4, 150 mM NaCl, 1 mM EDTA, 1% Triton X100) containing fresh 1 mM PMSF and protease inhibitors (Roche). The samples were quantified by Bradford assay, denatured by boiling in Laemmli buffer, and total protein was separated

by SDS-PAGE. After transfer to the PVDF membrane (Bio-Rad) and blocking with Odyssey Blocking Buffer (LI-COR), primary antibodies were incubated overnight at 4°C. Rabbit monoclonal anti-ERG antibody (Epitomics 2805-1) and rabbit polyclonal anti-actin antibody (Sigma A2066) were used. Goat anti-rabbit near-IR conjugated secondary antibody (LI-COR) was added and the bands were visualized on an Odyssey infrared imager (LI-COR). The experiment was conducted in duplicate and the data are representative of both trials.

Cellular uptake studies.

For visualization of uptake using FITC-analog polyamides, VCaP cells were plated in 35-mm optical dishes (MatTek) at 7.5×10^4 cells per dish and allowed to adhere for 48 h. Media was then changed and cells were treated with 0.1% DMSO with polyamide for 24 or 48 h. Cells were then imaged at the Caltech Beckman Imaging Center using a Zeiss LSM 5 Exciter inverted laser scanning microscope equipped with a 63x oil immersion lens as previously described (39).

WST-1 proliferation assay.

VCaP cells were plated at 1×10^3 per well in 96-well plates coated with poly-L-lysine (BD BioCoat). After 24 h, an additional volume of medium containing vehicle or polyamide was added to each well. All medium was removed following 72 h of polyamide incubation and replaced with one volume of WST-1 reagent (Roche) in medium according to manufacturer protocol. After 4 h of incubation at 37°C, the absorbance was measured on a FlexStation3 plate reader (Molecular Devices). The value

of A(450nm)-A(630nm) of treated cells was referenced to vehicle treated cells. Non-linear regression analysis (Prism software, Graphpad) was performed to determine IC₅₀ values.

HUVEC tube formation.

HUVEC cells were plated at a density of 2×10^5 cells per 75 cm flask in 200 PRF medium (Gibco) supplemented with Low Serum Growth Supplement (LSGS, Invitrogen). After 36 h, polyamides were added to a concentration of 10 μ M, and the cells were incubated for 72 h. The cells were then trypsinized and 8×10^4 cells/well were plated in 12-well plates coated with 100 μ L of solidified Geltrex reduced growth factor basement membrane (Invitrogen). After 6 h the wells were imaged on an inverted microscope equipped with a 5x objective by selecting four random fields of view between two wells per treatment condition. Data was analyzed by manually counting the number of sprouts in each field of view.

Single cell electrophoresis (COMET) assay.

VCaP cells (3×10^6 cells) were plated in 10 cm cell culture dishes and allowed to adhere for 24 h before addition of DMSO vehicle or polyamide stock in DMSO. After 72 h incubation, cells were washed with warm PBS (37°C), gently scraped, and counted. Samples were centrifuged, resuspended at 1×10^5 cells/mL, and treated according to manufacturer protocol (Trevigen) for neutral electrophoresis. Slides were stained with SybrGreen (Trevigen) and imaged at the Caltech Beckman Imaging Center using a Zeiss LSM 5 Pascal inverted laser scanning microscope equipped with a 5x air objective lens.

Overlaid fluorescence and bright field images were obtained using standard filter sets for fluorescein. Images were analyzed using COMET IV software (Perceptive Instruments Ltd) with 200-600 comets measured per sample. A random sampling of 200 comets per condition was used for two-way ANOVA analysis (Prism software, GraphPad) of three biological replicates.

Xenograft assays.

SCID mice (4-6 weeks old) were injected above the right flank with 1×10^6 VCaP cells (10 mice per dose group). Tumor was measured by caliper until the tumor size reached 100 mm^3 . All mice were treated subcutaneously with control (DMSO) or with doses of polyamides as reported (3 times per week, 10 total injections). Tumor growth was followed weekly by caliper measurements (40).

4.5 Acknowledgments

The authors would like to thank Prof. Arul M. Chinnaiyan (University of Michigan) for the VCaP cell line, and J. Chad Brenner (University of Michigan) for helpful discussions.

4.6 References

1. Rubin, M.A. (2012) ETS rearrangements in prostate cancer. *Asian J Androl*, 14, 393-399.
2. Perner, S., Demichelis, F., Beroukhi, R., Schmidt, F.H., Mosquera, J.M., Setlur, S., Tchinda, J., Tomlins, S.A., Hofer, M.D., Pienta, K.G. *et al.* (2006) TMPRSS2:ERG fusion-associated deletions provide insight into the heterogeneity of prostate cancer. *Cancer research*, 66, 8337-8341.
3. Demichelis, F., Fall, K., Perner, S., Andren, O., Schmidt, F., Setlur, S.R., Hoshida, Y., Mosquera, J.M., Pawitan, Y., Lee, C. *et al.* (2007) TMPRSS2:ERG gene fusion associated with lethal prostate cancer in a watchful waiting cohort. *Oncogene*, 26, 4596-4599.
4. Attard, G., Clark, J., Ambrosini, L., Fisher, G., Kovacs, G., Flohr, P., Berney, D., Foster, C.S., Fletcher, A., Gerald, W.L. *et al.* (2008) Duplication of the fusion of TMPRSS2 to ERG sequences identifies fatal human prostate cancer. *Oncogene*, 27, 253-263.
5. Tomlins, S.A., Rhodes, D.R., Perner, S., Dhanasekaran, S.M., Mehra, R., Sun, X.W., Varambally, S., Cao, X., Tchinda, J., Kuefer, R. *et al.* (2005) Recurrent fusion of TMPRSS2 and ETS transcription factor genes in prostate cancer. *Science (New York, N.Y.)*, 310, 644-648.
6. Perner, S., Mosquera, J.M., Demichelis, F., Hofer, M.D., Paris, P.L., Simko, J., Collins, C., Bismar, T.A., Chinnaiyan, A.M., De Marzo, A.M. *et al.* (2007) TMPRSS2-ERG fusion prostate cancer: an early molecular event associated with invasion. *The American journal of surgical pathology*, 31, 882-888.
7. Brenner, J.C., Ateeq, B., Li, Y., Yocum, A.K., Cao, Q., Asangani, I.A., Patel, S., Wang, X., Liang, H., Yu, J. *et al.* (2011) Mechanistic Rationale for Inhibition of Poly(ADP-Ribose) Polymerase in ETS Gene Fusion-Positive Prostate Cancer. *Cancer Cell*, 19, 664-678.
8. Carver, B.S., Tran, J., Gopalan, A., Chen, Z., Shaikh, S., Carracedo, A., Alimonti, A., Nardella, C., Varmeh, S., Scardino, P.T. *et al.* (2009) Aberrant ERG expression cooperates with loss of PTEN to promote cancer progression in the prostate. *Nature genetics*, 41, 619-624.
9. King, J.C., Xu, J., Wongvipat, J., Hieronymus, H., Carver, B.S., Leung, D.H., Taylor, B.S., Sander, C., Cardiff, R.D., Couto, S.S. *et al.* (2009) Cooperativity of TMPRSS2-ERG with PI3-kinase pathway activation in prostate oncogenesis. *Nature genetics*, 41, 524-526.
10. Dervan, P.B. (2001) Molecular recognition of DNA by small molecules. *Bioorgan Med Chem*, 9, 2215-2235.

11. Dervan, P.B. and Edelson, B.S. (2003) Recognition of the DNA minor groove by pyrrole-imidazole polyamides. *Current Opinion in Structural Biology*, 13, 284-299.
12. Chenoweth, D.M. and Dervan, P.B. (2010) Structural Basis for Cyclic Py-Im Polyamide Allosteric Inhibition of Nuclear Receptor Binding. *J Am Chem Soc*, 132, 14521-14529.
13. Olenyuk, B.Z., Zhang, G.-J., Klco, J.M., Nickols, N.G., Kaelin, W.G., Jr. and Dervan, P.B. (2004) Inhibition of vascular endothelial growth factor with a sequence-specific hypoxia response element antagonist. *Proceedings of the National Academy of Sciences of the United States of America*, 101, 16768-16773.
14. Nickols, N.G. and Dervan, P.B. (2007) Suppression of androgen receptor-mediated gene expression by a sequence-specific DNA-binding polyamide. *Proceedings of the National Academy of Sciences of the United States of America*, 104, 10418-10423.
15. Nickols, N.G., Jacobs, C.S., Farkas, M.E. and Dervan, P.B. (2007) Modulating hypoxia-inducible transcription by disrupting the HIF-1-DNA interface. *ACS Chemical Biology*, 2, 561-571.
16. Muzikar, K.A., Nickols, N.G. and Dervan, P.B. (2009) Repression of DNA-binding dependent glucocorticoid receptor-mediated gene expression. *Proceedings of the National Academy of Sciences of the United States of America*, 106, 16598-16603, S16598/16591-S16598/16596.
17. Raskatov, J.A., Meier, J.L., Puckett, J.W., Yang, F., Ramakrishnan, P. and Dervan, P.B. (2012) Modulation of NF-kappaB-dependent gene transcription using programmable DNA minor groove binders. *Proceedings of the National Academy of Sciences of the United States of America*, 109, 1023-1028.
18. Raskatov, J.A., Nickols, N.G., Hargrove, A.E., Marinov, G.K., Wold, B. and Dervan, P.B. (2012) Gene expression changes in a tumor xenograft by a pyrrole-imidazole polyamide. *Proceedings of the National Academy of Sciences of the United States of America*, 109, 16041-16045.
19. Nickols, N.G., Szablowski, J.O., Hargrove, A.E., Li, B.C., Raskatov, J.A. and Dervan, P.B. (2013) Activity of a py-im polyamide targeted to the estrogen response element. *Molecular cancer therapeutics*, 12, 675-684.
20. Wang, X., Nagase, H., Watanabe, T., Nobusue, H., Suzuki, T., Asami, Y., Shinojima, Y., Kawashima, H., Takagi, K., Mishra, R. *et al.* (2010) Inhibition of MMP-9 transcription and suppression of tumor metastasis by pyrrole-imidazole polyamide. *Cancer science*, 101, 759-766.

21. Yang, F., Nickols, N.G., Li, B.C., Marinov, G.K., Said, J.W. and Dervan, P.B. (2013) Antitumor activity of a pyrrole-imidazole polyamide. *Proc Natl Acad Sci U S A*, 110, 1863-1868.
22. Raskatov, J.A., Hargrove, A.E., So, A.Y. and Dervan, P.B. (2012) Pharmacokinetics of Py-Im Polyamides Depend on Architecture: Cyclic versus Linear. *J Am Chem Soc*, 134, 7995-7999.
23. Synold, T.W., Xi, B., Wu, J., Yen, Y., Li, B.C., Yang, F., Phillips, J.W., Nickols, N.G. and Dervan, P.B. (2012) Single-dose pharmacokinetic and toxicity analysis of pyrrole-imidazole polyamides in mice. *Cancer chemotherapy and pharmacology*, 70, 617-625.
24. Yang, F., Nickols, N.G., Li, B.C., Szablowski, J.O., Hamilton, S.R., Meier, J.L., Wang, C.M. and Dervan, P.B. (2013) Animal toxicity of hairpin pyrrole-imidazole polyamides varies with the turn unit. *J Med Chem*, 56, 7449-7457.
25. Tomlins, S.A., Laxman, B., Varambally, S., Cao, X., Yu, J., Helgeson, B.E., Cao, Q., Prensner, J.R., Rubin, M.A., Shah, R.B. *et al.* (2008) Role of the TMPRSS2-ERG gene fusion in prostate cancer. *Neoplasia*, 10, 177-188.
26. Yu, J.D., Yu, J.J., Mani, R.S., Cao, Q., Brenner, C.J., Cao, X.H., Wang, X.J., Wu, L.T., Li, J., Hu, M. *et al.* (2010) An Integrated Network of Androgen Receptor, Polycomb, and TMPRSS2-ERG Gene Fusions in Prostate Cancer Progression. *Cancer Cell*, 17, 443-454.
27. Brenner, J.C., Feng, F.Y., Han, S., Patel, S., Goyal, S.V., Bou-Maroun, L.M., Liu, M., Lonigro, R., Prensner, J.R., Tomlins, S.A. *et al.* (2012) PARP-1 inhibition as a targeted strategy to treat Ewing's sarcoma. *Cancer research*, 72, 1608-1613.
28. Birdsey, G.M., Dryden, N.H., Amsellem, V., Gebhardt, F., Sahnian, K., Haskard, D.O., Dejana, E., Mason, J.C. and Randi, A.M. (2008) Transcription factor Erg regulates angiogenesis and endothelial apoptosis through VE-cadherin. *Blood*, 111, 3498-3506.
29. Berger, M.F., Lawrence, M.S., Demichelis, F., Drier, Y., Cibulskis, K., Sivachenko, A.Y., Sboner, A., Esgueva, R., Pflueger, D., Sougnez, C. *et al.* (2011) The genomic complexity of primary human prostate cancer. *Nature*, 470, 214-220.
30. Mounir, Z., Lin, F., Lin, V.G., Korn, J.M., Yu, Y., Valdez, R., Aina, O.H., Buchwalter, G., Jaffe, A.B., Korpai, M. *et al.* (2014) TMPRSS2:ERG blocks neuroendocrine and luminal cell differentiation to maintain prostate cancer proliferation. *Oncogene*.
31. Martinez, T.F., Phillips, J.W., Karanja, K.K., Polaczek, P., Wang, C.M., Li, B.C., Campbell, J.L. and Dervan, P.B. (2014) Replication stress by Py-Im polyamides

- induces a non-canonical ATR-dependent checkpoint response. *Nucleic Acids Res*, 42, 11546-11559.
32. Raskatov, J.A., Nickols, N.G., Hargrove, A.E., Marinov, G.K., Wold, B. and Dervan, P.B. (2012) Gene expression changes in a tumor xenograft by a pyrrole-imidazole polyamide. *Proc Natl Acad Sci U S A*, 109, 16041-16045.
 33. Raskatov, J.A., Szablowski, J.O. and Dervan, P.B. (2014) Tumor xenograft uptake of a pyrrole-imidazole (Py-Im) polyamide varies as a function of cell line grafted. *J Med Chem*, 57, 8471-8476.
 34. Puckett, J.W., Green, J.T. and Dervan, P.B. (2012) Microwave Assisted Synthesis of Py-Im Polyamides. *Org. Lett.*, 14, 2774-2777.
 35. Nickols, N.G., Jacobs, C.S., Farkas, M.E. and Dervan, P.B. (2007) Improved nuclear localization of DNA-binding polyamides. *Nucleic Acids Research*, 35, 363-370.
 36. Dose, C., Farkas, M.E., Chenoweth, D.M. and Dervan, P.B. (2008) Next Generation Hairpin Polyamides with (R)-3,4-Diaminobutyric Acid Turn Unit. *J Am Chem Soc*, 130, 6859-6866.
 37. Li, B.C., Montgomery, D.C., Puckett, J.W. and Dervan, P.B. (2013) Synthesis of cyclic Py-Im polyamide libraries. *The Journal of organic chemistry*, 78, 124-133.
 38. Meier, J.L., Montgomery, D.C. and Dervan, P.B. (2011) Enhancing the cellular uptake of Py-Im polyamides through next-generation aryl turns. *Nucleic Acids Research*, 40, 2345-2356.
 39. Best, T.P., Edelson, B.S., Nickols, N.G. and Dervan, P.B. (2003) Nuclear localization of pyrrole-imidazole polyamide-fluorescein conjugates in cell culture. *Proceedings of the National Academy of Sciences of the United States of America*, 100, 12063-12068.
 40. McGregor, N., Patel, L., Craig, M., Weidner, S., Wang, S. and Pienta, K.J. (2010) AT-101 (R-(-)-gossypol acetic acid) enhances the effectiveness of androgen deprivation therapy in the VCaP prostate cancer model. *J. Cell. Biochem.*, 110, 1187-1194.